Math Geosci (2013) 45:621–645
DOI 10.1007/s11004-013-9467-0

SPECIAL ISSUE

Stochastic Simulation of Nonstationary Rainfall Fields, Accounting for Seasonality and Atmospheric Circulation Pattern Evolution

Gonzalo Sapriza Azuri · Jorge Jódar · Jesús Carrera · Hoshin V. Gupta

Received: 14 December 2012 / Accepted: 15 May 2013 / Published online: 2 July 2013

Abstract A model for generating daily spatial correlated rainfall fields suitable for evaluating the impacts of climate change on water resources is presented. The model, termed Stochastic Rainfall Generating Process, is designed to incorporate two major nonstationarities: changes in the frequencies of different precipitation generating mechanisms (frontal and convective), and spatial nonstationarities caused by interactions of mesoscale atmospheric patterns with topography (orographic effects). These nonstationarities are approximated as discrete sets of the time-stationary Stochastic Rainfall Generating Process, each of which represents the different spatial patterns of rainfall (including its variation with topography) associated with different atmospheric circulation patterns and times of the year (seasons). Each discrete Stochastic Rainfall Generating Process generates daily correlated rainfall fields as the product of two random fields. First, the amount of rainfall is generated by a transformed Gaussian process applying sequential Gaussian simulation. Second, the delimitation of rain and no-rain areas (intermittence process) is defined by a binary random function simulated by sequential indicator simulations. To explore its applicability, the model is tested in the Upper Guadiana Basin in Spain. The result suggests that the model provides accurate reproduction of the major spatiotemporal features of rainfall needed for hydrological modeling and water resource evaluations. The results were

G. Sapriza Azuri (✉)
GHS, Department of Geotechnical Engineering and Geoscience, Technical University of Catalonia, Barcelona, Spain
e-mail: gonzalo.sapriza@upc.edu

G. Sapriza Azuri · J. Jódar · J. Carrera
GHS, Institute of Environmental Assessment and Water Research (IDAEA), CSIC, Barcelona, Spain

J. Jódar
Hydromodel Host., Sant Joan de La Salle 42, Technova Building 3-12, 08022 Barcelona, Spain

H.V. Gupta
Department of Hydrology and Water Resources, University of Arizona, Tucson, AZ, USA

significantly improved by incorporating spatial drift related to orographic precipitation into the model.

Keywords Rainfall · Non-stationarity · Atmospheric circulation · Downscaling

1 Introduction

Climate Change Impact Studies (CCIS) rely upon simulations of past, present, and potential future climate scenarios provided by General Circulation Models (GCMs) (Randall et al. 2007; CCSP 2008). However, these simulations do not provide rainfall fields at the high spatial resolution generally required for hydrological impact assessments (Maraun et al. 2010). GCMs currently have a spatial discretization of around 250 km, whereas the resolution of hydrological models typically ranges from 2 km to 50 m. Moreover, simulated rainfall intensities are often significantly biased and fail to reproduce patterns of long-term variability (Dai 2006; Gleckler et al. 2008; CCSP 2008; Ehret et al. 2012; Johnson and Sharma 2011). To overcome these limitations, Stochastic Rainfall Models (SRMs), also known as Statistical Downscaling Models, have been recently developed (Fowler et al. 2007; Maraun et al. 2010). Such models seek to simulate the most important non-stationarities of rainfall while incorporating relevant information provided by GCMs (Hay et al. 1991; Bardossy and Plate 1992; Goodess and Palutikof 1998; Corte-Real et al. 1999; Bellone et al. 2000; Fowler et al. 2000, 2005; Yang et al. 2010). Furthermore, there is a growing interest in being able to simulate spatially distributed rainfall fields at any spatiotemporal scale required (Maraun et al. 2010). Four main types of SRM are discussed in the literature: (1) Multivariate Stochastic Rainfall Models (MSRMs), (2) Point Process Models (PPMs), (3) Random Cascade Models (RCMs), and (4) Transformed Gaussian Process Models (TGPMs). Each of these approaches has strengths and weaknesses. MSRMs provide the ability to simulate precipitation at a fixed set of locations by interpolating values across the domain; examples include autoregressive models (Bardossy and Plate 1992), generalized linear models (Chandler and Wheater 2002; Yang et al. 2005), multi-site Markov models (Wilks 1998), nonparametric multisite models (Buishand and Brandsma 2001), and reshuffling approach models (Mehrotra and Sharma 2009). PPMs have the ability to simulate rainfall at a very high temporal resolution (Waymire et al. 1984; Rodríguez-Iturbe et al. 1986; Cowpertwait 1995, 2010; Northrop 1998, Wheater et al. 2005; Zhang and Switzer 2007; Burton et al. 2010) but need large amounts of high quality data for model calibration.

RCMs arise from the study of scale-invariance of rainfall (Schertzer and Lovejoy 1987; Gupta and Waymire 1993) and apply multiplicative random cascade models in space and time (Jothityangkoon et al. 2000; Kang and Ramirez 2010). They can incorporate both climate information and the orographic effects on rainfall (Perica and Foufoula-Georgiou 1996; Ebtehaj and Foufoula-Georgiou 2010). Although such models are parsimonious and can reproduce characteristics such as spatiotemporal intermittence and clustering, they require long sequences of radar images that may

not always be available. Finally, the TGPM approach assumes that rainfall can be represented as a transformed multi-Gaussian stochastic process (Mejía and Rodríguez-Iturbe 1974; Bell 1987; Shah et al. 1996; Guillot 1999; Lanza 2000; De Oliveira 2004; Kyriakidis et al. 2004; Teo and Grimes 2007), conditioned on the knowledge of spatial average rainfall (Onibon et al. 2004) within a generalized linear model framework (Kleiber et al. 2012). One advantage of this approach is its ability to exploit information from either rain gauges or radar images. Models within this group differ in terms of the transformation used to generate a multidimensional stationary Gaussian process, the type of algorithm used to generate spatial realizations of rainfall, and the way in which rainfall intermittence is represented. Nevertheless, none of these models incorporate the major sources of nonstationarity in rainfall processes within a common framework. While consideration of spatial nonstationarity including climate information (only specific humidity) was incorporated by Kyriakidis et al. (2004), they did not explicitly represent the spatial intermittence of rainfall and focused only on conditional simulations. Meanwhile, Bell (1987), Guillot (1999), Lanza (2000), De Oliveira (2004) and Teo and Grimes (2007) explicitly included spatial intermittence of rainfall via threshold transformation or Sequential Indicator Simulation, but did not incorporate other sources of nonstationarity (i.e., orographic effect, climate).

To generate non-stationary stochastic rainfall fields suitable for evaluating the impacts of climate change on water resources, it is necessary to represent two major nonstationarities—changes in the frequencies of different precipitation generating mechanisms (frontal and convective) and spatial nonstationarities caused by interactions of mesoscale atmospheric patterns with topography (orographic effects) (Barros and Lettenmaier 1994). This paper introduces a new TGP termed Stochastic Rainfall Generating Process (SRGP) designed to simulate such nonstationarity in daily rainfall fields in the context of downscaling relevant climate information from GCMs. Instead of being based on GCM simulations of rainfall which are typically poor, SRGP takes advantage of the fact that GCMs are able to generate good simulations of other hydrometeorological variables (Gleckler et al. 2008) and, in particular, of atmospheric circulation patterns (ACP) at the synoptic scale (Randall et al. 2007). The methodology was developed using data from the Upper Guadiana basin in central Spain.

2 Methodology

In general, SRGP is a two-part model (Stern and Coe 1984). The first part decides whether a day is rainy or not, over the entire area of interest, while the second part deals with the manner in which the spatiotemporal pattern of rainfall is generated. The rain/no-rain decision can be made in the context of climate impact studies, on the basis of information GCM outputs or stochastic simulation using, for example, a first or second order Markov Chain Model or any of its variants (Sharma and Mehrotra 2010). The spatiotemporal rainfall pattern can be generated using a stochastic model designed to reproduce the observed spatial correlation structure of rainfall. However, it is well known that the spatiotemporal patterns of rainfall intensity vary with changes in temperature, and with changes in the velocity and direction of winds (and

their interactions with local topography and landscape), all of which vary throughout the year with changes in the regional atmospheric circulation patterns over the area. Our approach, therefore, is to assume that the overall non-stationary SRGP can be approximated by a time sequence of draws from a discrete set of time-stationary SRGPs, each of which represents the spatial patterns of rainfall (including its variation with topography) associated with different ACPs and seasons of the year. More specifically, the discrete set is constructed by classifying days according to (a) the ACP type for that day, and (b) the time of year (either month or season).

This results in a three-part SRGP model: (1) select the prevalent ACP, (2) decide whether the day is rainy or not and (3) simulate the spatial rainfall field. Again, each of these decisions can be made via stochastic simulation, provided that the probability of rain in the second stage depends on the selected ACP and time of year. Although conditional probability Markov chain models of this type can be easily constructed from observed data, including long term variability in their construction (Mehrotra and Sharma 2007, 2010), our attention here is focused on climate impact studies, in which case both the regional ACP type and rain/no-rain information for a day can be provided by a GCM with proper post processing to handle the rain no-rain transition (Johnson and Sharma 2011, 2012). Therefore, in this paper to further explore the rainfall field generation processes, we assume that the daily sequence of ACP types and whether a day is rainy or not are given. Based on this information, an appropriate SRGP model for the particular time of year (month or season) is selected from the discrete set. Consequently, the overall SRGP model is based on climatological information from three spatial scales—the synoptic scale (embodied through atmospheric circulation patterns), the basin scale (embodied through orographic effects and the spatial correlation structure of observed rainfall), and the point scale (embodied through rain-gauge measurements). Meanwhile, the model assumes that the temporal day-to-day persistence and the correlation structure of (catchment-scale) mean areal rainfall are largely determined by the (externally determined) ACP and rain-no-rain sequence with the result that daily persistence effects within and across ACP types can be ignored. While such effects could certainly also be modeled and reproduced, we leave such investigation for future studies.

2.1 The Problem of Simulating Stochastic Rainfall Fields

The main aim here is to simulate daily precipitation fields that reproduce the observed rainfall multidimensional cumulative distribution function (*mcdf*) at any desired spatial resolution. Of course, characterization of this *mcdf* is not trivial since it is (in general) nonstationary in space and time, has an unknown covariance structure, and depends on an unknown number of parameters. Let $z(u,t)$ denote a random value indicating the intensity of rain at a specific location in space (u) and time (t). This variable can be interpreted as a realization of a random variable $Z(u,t)$, which is characterized by the **c**umulative **d**istribution **f**unction (*cdf*)

$$F(u,t;z) = \Pr\{Z(u,t) \leq z\}. \tag{1}$$

The set of all the dependent random variables define a spatiotemporal random function $Z(u,t)$ that is totally characterized by its *mcdf* (Goovaerts 1997) given by

$$F_A\big(Z(u,\mathrm{t})\big) = F_A(u_1,t_1,\ldots,u_N,t_N;z_{11},\ldots,z_{NT}) = \Pr\big\{Z(u_1,t_1)\le z_{11},\ldots,Z(u_N,t_T)\le z_{NT}\big\}, \quad (2)$$

where N and T are the total number of points in the spatial and temporal domain, respectively. This function has an arbitrary mathematical form (Kyriakidis and Journel 1999). For rainfall, the random function (*RF*) can be regarded as being composed of two terms (1) a continuous random function $R(u,t)$ representing its intensity and (2) a categorical random function $I(u,t)$ representing its space-time intermittence

$$F_A\big(Z(u,t)\big) = F_A\big(R(u,t),I(u,t)\big). \quad (3)$$

To model this random function, it is necessary to make assumptions about (a) the main causes of temporal nonstationarity in the rainfall generating process, (b) the spatial rainfall mean and variance, (c) the probability distribution function of rainfall intensity, (d) the causes of spatial non-stationarity in rainfall intensity, and (e) the structure of spatial intermittence.

2.1.1 Main Causes of Temporal Nonstationarity

As stated above, it is assumed here that the major causes of temporal non-stationarity in the rainfall generating process are its dependence on (1) seasonal variations in the climatological variables, (2) synoptic scale atmospheric factors (circulation patterns; Bardossy and Plate 1992; Hay et al. 1991; Corte-Real et al. 1999; Bellone et al. 2000; Fowler et al. 2000, 2005; Yang et al. 2010), and (3) interactions between atmospheric conditions and local factors such as topographic slope and aspect (Barros and Lettenmaier 1994). Accordingly, we assume that $F_A(Z(u,t))$ can be approximated by a discrete set of N SRGPs $\{F_{A_1}(Z(u,t)),\ldots,F_{A_N}(Z(u,t))\}$, in such a way that each day corresponds only to one SGPR and where each member $F_{A_j}(Z(u,t))$ is assumed to be stationary in time, but may be nonstationary in space. Consequently, temporal changes in the rainfall regime (the spatial distribution of rainfall intensities) are due primarily to changes in the sequence of SRGPs with the result that the functional form of each SRGP is conditionally independent. This means that the temporal correlation in the rainfall regime arises primarily from the correlation in the daily sequence of SRGP occurrences, and the daily spatial distributions are assumed (for simplicity) to be temporally independent. Hence, the rainfall field on any day is assumed to be conditionally independent of the rainfall field on any previous day. This does not mean, however, that the daily sequence of rainfall fields has no temporal dependence since a temporal relationship exists in the sequence of the different SRGPs because of the temporal evolution in synoptic scale atmospheric circulation patterns.

2.1.2 Spatial Rainfall Mean and Variance

For a given SRGP, the strength of the link between the synoptic and the basin scales can be quantified by characterizing the daily spatial rainfall mean (Eq. (4)) and variance (Eq. (5)) with respect to the predominant atmospheric synoptic scenario

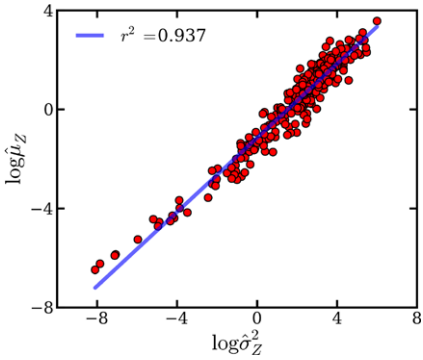

Fig. 1 Example of empirical relationship between spatial average and variance of rainfall for rainy days of April and May that belong to the HYC ACP type. *Red dots* denote observations

$$\hat{\mu}_{Z_j}(t) = \frac{1}{N_j}\sum_{i=1}^{N_j} z_i(t), \quad j = 1, \ldots, N, \tag{4}$$

$$\hat{\sigma}^2_{Z_j}(t) = \frac{1}{N_j}\sum_{i=1}^{N_j} \big(z_i(t) - \hat{\mu}_{Z_j}\big)^2, \quad j = 1, \ldots, N, \tag{5}$$

where N_j is the number of rain gauge stations for a day belonging to the jth SRGP. Here, we assume temporal disaggregation of rainfall intensities (the sequence of rainy days is time independent and controlled by the daily transition of ACPs), which allows us to estimate the spatial daily average and variance of rainfall by obtaining their respective Probability Distribution Functions (*pdfs*) for each SRGP. However, as might be expected, $\hat{\sigma}^2_{Z_j}(t)$ and $\hat{\mu}_{Z_j}(t)$ are not independent. In the case study (Sect. 6), a strong linear dependence between the log transformed values is observed (Fig. 1); such that we can express $\hat{\sigma}^2_{Z_j}(t)$ as a function of $\hat{\mu}_{Z_j}(t)$ by fitting a linear regression model

$$\log\hat{\sigma}^2_{Z_j}(t) = m_{Z_j}\log\hat{\mu}_{Z_j}(t) + c_{Z_j}. \tag{6}$$

Several possibilities for the *pdf* of $\hat{\mu}_{Z_j}(t)$ have been proposed in the literature including the lognormal distribution (Kedem and Chiu 1987), gamma distribution (Cho et al. 2004), GLM (Stern and Coe 1984), and more recently a class termed the infinitely divisible distribution (Kundu and Siddani 2007). Here, we assume a gamma distribution (Eq. (7)) because of its parsimony in the number of parameters

$$\Gamma_{\hat{\mu}_{Z_j}}(\alpha_j, \beta_j) = \frac{(\frac{\hat{\mu}_{Z_j}}{\beta_j})^{\alpha-1} e^{-\frac{\hat{\mu}_{Z_j}}{\beta_j}}}{\beta_j \Gamma(\alpha_j)}, \tag{7}$$

where α and β are the shape and the scale parameters, respectively. To estimate them a maximum likelihood approach was applied, obtaining the relatively good fit shown in Fig. 2.

2.1.3 Probability Distribution Function of Rainfall Intensity

The rainfall intensity $\{R_j(u,t)\}$ random function for each SRGP has an unknown multidimensional distribution shape F_{R_j}, which is clearly not multi-Gaussian. To take

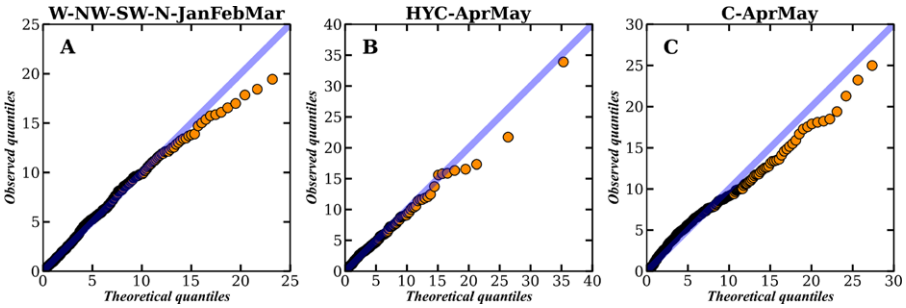

Fig. 2 Quantile–Quantile plots illustrating Gamma distribution fits to spatial average rainfall. There are for days associated with the rainiest *season–ACP* combination in the Upper Guadiana Basin. (**A**) Directional W–NW–SW–N in January, February, and March, (**B**) Hybrid Cyclonic in April and May, and (**C**) Cyclonic in April and May

advantage of the theory of Gaussian random processes, we therefore transform each rainfall intensity *mcdf* into a multi-Gaussian distribution by applying a normal score transformation (also known as quantile–quantile mapping or anamorphosis transformation) (Goovaerts 1997). In practice, we first compute the standardized daily rainfall amount $Y_j(u,t)$ as follows:

$$Y_j(u,t) = \frac{R_j(u,t) - \hat{\mu}_{Z_j}(t)}{\hat{\sigma}_{Z_j}(t)}, \tag{8}$$

and then perform the normal score transformation by establishing a quantile–quantile mapping between the *cdf* of all the standardized rainfall intensity measurements $Y_j(u,t)$ for the SRGP and the *cdf* of a standardized Gaussian distribution in order to obtain

$$\psi_j(u,t) = G^{-1}_{\psi_j}\big(F_{Y_j}\big(Y_j(u,t)\big)\big), \tag{9}$$

where $\psi_j(u,t)$ is the new normal scored variable, $G^{-1}_{\psi_j}$ is the inverse Gaussian *cdf* of $\psi_j(u,t)$, and F_{Y_j} is the *cdf* of $Y_j(u,t)$.

2.1.4 Spatial Nonstationarity in Rainfall Intensity

Rainfall intensity can be spatially nonstationary due to local factors such as topography, agricultural irrigation, urbanization, and more. To represent such spatial nonstationarities, we consider $\psi_j(u,t)$ to be an intrinsic stationary function composed of a trend and a residual

$$\psi_j(u,t) = \overline{\psi}_j(u) + \xi_j(u,t) \tag{10}$$

is used where $\overline{\psi}_j(u)$ represents the deterministic dependence of rainfall intensity on external factors (known as the trend term), and a residual $\xi_j(u,t)$, which is a zero-mean Gaussian random function whose spatial correlation structure is described by a semivariogram $\gamma_{\xi_j}(u)$ (termed variogram hereafter). In this study, we assume that rainfall intensity varies only with topographic elevation and estimate the trend term

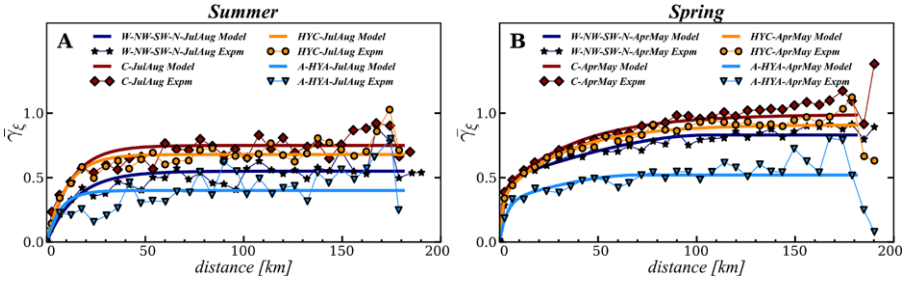

Fig. 3 Experimental and model semivariograms for Summer (**A**) and Spring (**B**) for the rainiest and most frequent ACPs (W–NW–SW–N, C, HYC, and A-HYA). The model semivariograms are isotropic, and in most cases, have two structural components, exponential and spherical

by linear regression. After removing the trend from $\psi_j(u,t)$, the variogram was experimentally inferred for each SRGP (Fig. 3). Given this model, spatial random fields at any desired resolution can be generated using **S**equential **G**aussian **S**imulation (SGS) (Gómez-Hernández and Cassiraga 1994; Deutsch and Journel 1997).

2.1.5 Structure of Spatial Intermittence

The rainfall intensity model described above will generate non-zero rainfall intensity values at all spatial locations where values are desired. However, the observed rainfall tends to be spatially intermittent (contiguous regions of zero and nonzero rainfall). To be realistic, the rainfall generation process must emulate the patterns of spatial intermittence, and in particular should reproduce the daily variation in the fraction of rain-covered area (Doneaud et al. 1984; Kedem and Pavlopoulos 1991; Eltahir and Bras 1993; Kursinski and Zeng 2006). Figure 4 shows an example of the dependence between spatial mean rainfall $\hat{\mu}_{Z_j}(t)$ and the fraction of rain-covered area $\theta_j(t)$ in our study area, to which an exponential curve of the following form can be fitted:

$$\theta_j(t) = a\big(1 - \exp\big(-b\hat{\mu}_{Zj}(t)\big)\big), \tag{11}$$

where a and b are the fitted parameters. To delimit the spatial extension of non-zero rainfall intensity, we assume that the simulated rainfall field $P_j(u,t)$ (Eq. (12)) is the combination of two independent random variables (Barancourt et al. 1992) being (1) the intensity of rainfall $R_j(u,t)$ and (2) a binary RF $I_j(u,t)$ representing spatial intermittence (Eq. (13)). The binary random field $I_j(u,t)$ is assumed to be stationary with a marginal probability equal to the fractional area covered by rain (Eq. (14)) and with a spatial correlation structure that is different for every. To simulate rainfall intermittence, a **S**equential **I**ndicator **S**imulation (SIS) approach with simple kriging is applied (Gómez-Hernández and Srivastava 1990; Deutsch and Journel 1997) in such a way that

$$P_j(u,t) = K_j(t)R_j(u,t)I_j(u,t), \tag{12}$$

$$I_j(u,t) = \begin{cases} 0 \to Z(u,t) = 0 & \text{for } t \in \text{SRGP}_j \\ 1 \to Z(u,t) > 0 & \text{for } t \in \text{SRGP}_j, \end{cases} \tag{13}$$

$$\theta_j(t) = E\big[I_j(u,t)\big]. \tag{14}$$

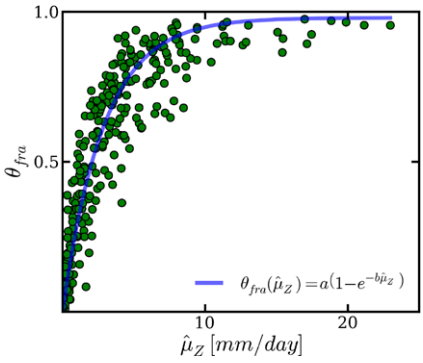

Fig. 4 Example of empirical relationship between spatial average rainfall and fraction of rain-covered area for the rainy days of January, February, and March that belong to the HYC ACP type. *Green dots* denote observations

The multiplying factor $K_j(t)$ in Eq. (12) is necessary to preserve the spatial mean intensity of rainfall $\hat{\mu}_{Z_j}(t)$, which is altered by the removal of areas assumed to have zero rain ($I_j(u,t)$).

2.2 Definition of the Atmospheric Circulation Patterns

One major characteristic of our method is its decomposition of the *mcdf* into N conditionally independent and temporally stationary SRGPs. This decomposition seeks to account for the dependence of the rainfall generating process on climatological and other (earth system process) factors. There are several ways to construct the mapping from $t \rightarrow j$, depending on the hypothesis made in regard to the dominant causes of temporal nonstationarity in $F_A(Z(u,t))$. In general, the dominant causes of this nonstationarity are (1) mesoscale and regional climatological processes such as ACPs and moisture convergence (Trenberth et al. 2003) and (2) earth system processes such as the interactions of the local atmospheric conditions with the topography and the direction of the prevailing winds (Jodar et al. 2010). One relatively simple way to incorporate climate information is to relate synoptic general circulation patterns to local scale precipitation ($F_A(Z(u,t))$). Such assumptions have been postulated and tested by Hay et al. (1991), Bardossy and Plate (1992), Perica and Foufoula-Georgiou (1996), Goodess and Palutikof (1998), Corte-Real et al. (1999), Bellone et al. (2000), Fowler et al. (2000, 2005), Yang et al. (2010) with some success. In our study, we implement a decomposition approach where the frequency of rainy days, the daily mean intensity of rain and the patterns of spatial rainfall are controlled by the frequency and seasonality of the ACPs over the study area. This requires a method for classifying atmospheric circulation patterns into a discrete set of consistent ACP types. For this study an automated version of the Lamb Weather Type classification scheme (Jenkinson and Collison 1977; Jones et al. 1993) is used in accordance with Goodess and Palutikof (1998), which is based on the direction of surface wind and on its vorticity in geostrophic units. For the study area, gridded values of mean sea level pressure at 16 points distributed over Spain are used, obtained from the gridded NCEP-NCAR reanalysis data set (Kalnay et al. 1996); the result is 8 ACP types (Table 1).

Table 1 Atmospheric circulation pattern classification

ACP type	Description
C	Cyclonic
HYC	Hybrid cyclonic
UC	Unclassified/light flow cyclonic
A/HYA	Anticyclonic/hybrid-anticyclonic
UA	Unclassified/light flow-anticyclonic
W/NW/SW/N	Westerly northwesterly/southwesterly/northerly directional types
E/NE	Easterly/northeasterly directional types
S/SE	Southerly/southeasterly directional types

3 Model Identification Procedure

The steps used to calibrate the stochastic rainfall generation model are as follows:

(1) Define the SRGP classification scheme. For example, classify ACPs using the modified Lamb Weather Type classification and group days by ACP and time of year (season or month).

Then, for each SRGP type:

(2) Compute the daily spatial mean $\hat{\mu}_{Z_j}(t)$ and variance $\hat{\sigma}^2_{Z_j}(t)$ (Eqs. (4) and (5)) of rainfall intensity by using all available weather stations (including the locations with zero values) for each rainy day (a day is considered to be rainy if there is at least one meteorological station in the study area with nonzero precipitation).
(3) Estimate the parameters of Eq. (6) relating $\hat{\mu}_{Z_j}(t)$ and $\hat{\sigma}^2_{Z_j}(t)$.
(4) Estimate $\hat{\mu}_{Z_j}(t)$ by fitting the gamma distribution function $\Gamma_{\hat{\mu}_{Z_j}}(\alpha_j, \beta_j)$ (Eq. (7)).
(5) Estimate the exponential regression parameters a and b of the functional relationship between the daily spatial mean intensity $\hat{\mu}_{Z_j}(t)$ and the daily fraction of rain-covered area $\theta_j(t)$ (Eq. (11)).
(6) Standardize the daily rainfall intensities (Eq. (8)).
(7) Apply the normal score transformation to the standardized rainfall (Eq. (9)).
(8) Estimate the trend between the standardized variable $\psi_j(u,t)$ and the elevation topography.
(9) Obtain the residuals $\xi_j(u,t)$ (Eq. (10)).
(10) Estimate the experimental daily variogram of the residuals $\gamma_{\xi_j}(u)$ for each day, compute the average and then fit the model variogram.
(11) Estimate the daily experimental variogram of the binary rainfall occurrence variable $\gamma_{I_j}(u)$ for each day, compute the average and then fit the model variogram.

4 Stochastic Simulation Procedure

The daily sequence of rainfall fields is simulated by applying the following steps:

(1) Obtain the daily sequence of SRGPs according to the classifying scheme chosen.
(2) Determine whether a day is rainy or not.
(3) For each rainy day t_n belonging to each SRGP$_j$, use SGS to generate $\xi_j(u, t_n)$ fields with the appropriate variogram $\overline{\gamma}_{\xi_j}(u)$.
(4) Add the trend component $\overline{\psi}_j(u)$ (Eq. (10)) to obtain $\psi_j(u, t_n)$.
(5) Obtain the $Y_j(u, t_n)$ fields by applying the inverse normal score function (Eq. (9)) to $\psi_j(u, t_n)$.
(6) Sample $\hat{\mu}_{Z_j}(t_n)$ from the gamma distribution and obtain the corresponding variance $\hat{\sigma}^2_{Z_j}(t_n)$ by applying Eq. (6).
(7) Obtain the rainfall intensity field $R_j(u, t_n)$ by adding $\hat{\mu}_{Z_j}(t_n)$ and multiplying by $\hat{\sigma}^2_{Z_j}(t_n)$ (Eq. (8)).
(8) Obtain the fraction of rain-covered area $\theta_j(t_n)$ for the given $\hat{\mu}_{Z_j}(t_n)$ by using Eq. (11).
9) Simulate the spatial intermittence binary field $I_j(u, t_n)$ applying SIS and using the appropriate variogram $\gamma_{I_j}(u)$ and the corresponding fraction of rain-covered area $\theta_j(t_n)$.
(10) Use (Eq. (12)) to compute the final rainfall field $P_j(u, t_n)$, where the multiplying factor $K_j(t_n)$ is computed so as to preserve the spatial mean of rainfall intensity selected in step 6.

5 Test Case Application

In the following section, the rainfall field simulation method is applied to the Upper Guadiana basin (UppGb) in Spain for the period of 1959 to 2007. The SRGP$_j$ parameters were estimated using daily rainfall data from meteorological stations located in the study area. The ACP classification was obtained by applying the Lamb Weather Type classification scheme to the NCEP-NCAR reanalysis data set (Kalnay et al. 1996).

5.1 Study Area

The UppGb forms part of the central Spanish Plateau, and covers an area of approximately 16000 km^2 (Fig. 5). The basin is located between latitudes 38°37′N and 40°08′N, and longitudes between 2°25′W and 3°51′W. Morphologically, the main part of the basin is characterized by a smooth topography with altitudes ranging from 550 to 700 m a.s.l. (above sea level). Nevertheless, the northern and southern boundaries (Sierra Altomira and Campos de Montiel, respectively) show a mountainous landscape with an altitude exceeding 1000 m a.s.l. The UppGb has a mixed continental, semiarid, Mediterranean climate. Precipitation has notable space-time variability because of Atlantic and Mediterranean influences and because of orographic effects. The mean areal annual precipitation in the basin is approximately 450 mm per year, but varies both spatially (recorded minimum and maximum gauges display means

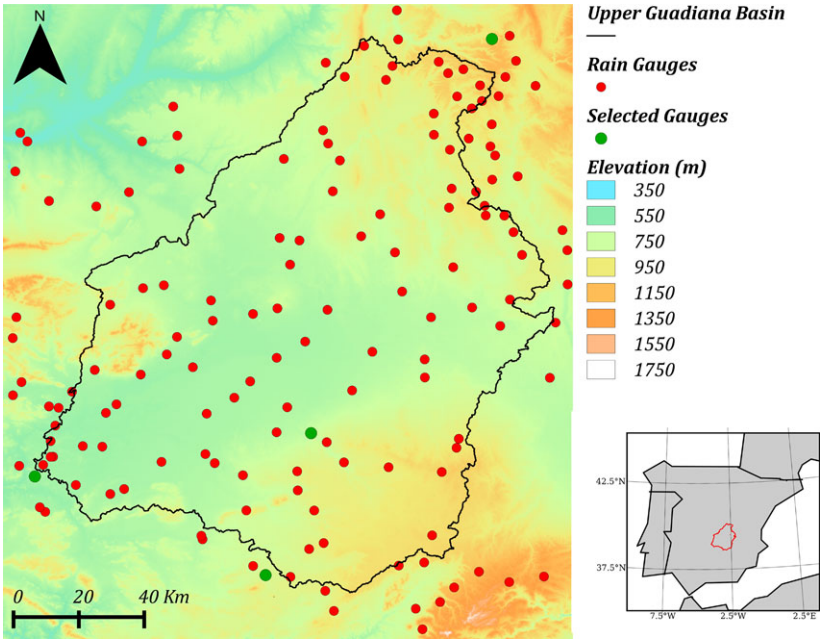

Fig. 5 Location of study area. The *black line* is the administrative limit of the Upper Guadiana Basin, and the *red dots* indicate locations of the meteorological stations

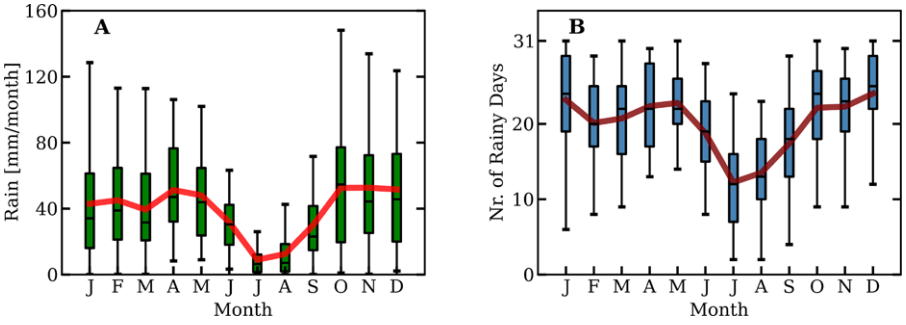

Fig. 6 Climatology plots for the Upper Guadiana Basin. (**A**) Spatial average rainfall, (**B**) Number of rainy days per month. A day is defined as rainy if at least one meteorological station reports daily measured rainfall exceeding zero

of 173 and 824 mm per year at the valley and mountains, respectively) and temporally (the standard deviation of the total yearly rainfall at the same stations are 121 and 233 mm per year, respectively). Its main characteristics are seasonal variability (Fig. 6) with a dry season in summer (especially in July and August which account for 5 % of the annual precipitation). This precipitation is dominated by small convective rain cells of short duration. The wettest seasons, autumn and spring, are characterized by stratiform frontal rain with large spatial continuity and duration. At point (rain gauge) scale, the number of dry days can be as high as 80 % on average (varying with the seasons), but this percentage drops to 50 % if we con-

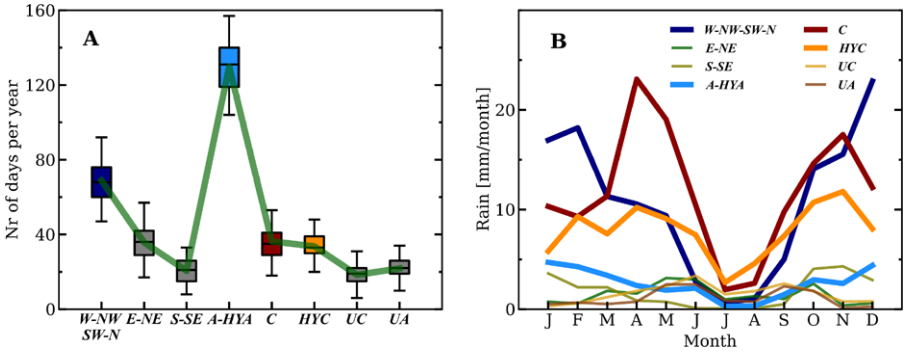

Fig. 7 Rainfall characteristics in the Upper Guadiana Basin for the different Atmospheric Circulation Patterns: (**A**) Average annual frequency of occurrence for each ACP type. (**B**) Climatology of spatial average rainfall for each ACP type (wetter ACPs are highlighted using *thicker lines*)

sider areal average rainfall, which suggests a high degree of spatial variability in the occurrence of precipitation. Orographic effects also contribute to spatial variability in rainfall intensities, with an average increase in precipitation with an elevation of around 0.0075 mm/m. Application of the ACP scheme indicates that higher rainfall amounts are associated with (1) the directional type ACP (W/NW/SW/N), which brings moisture from the Atlantic ocean, (2) the cyclonic C and hybrid-cyclonic types HYC, which are associated with low pressure systems, and (3) the anticyclonic A and hybrid-anticyclonic types A-HYA, which are associated with high pressure systems (Fig. 7). Figure 7b shows the mean annual volume of rainfall associated with the study area for each ACP type. One very important feature is the climatological pattern of rainfall for each ACP. This pattern must be properly reproduced by the selected hypothesis regarding the classification of the nonstationary rainfall process.

6 Results

Our evaluation of the performance of the proposed method is made from two perspectives: (1) reproduction of climatology and (2) reproduction of the spatial distribution of rainfall. In addition, an example of how well the intermittence process is reproduced is presented. Eleven conceptual models regarding the non-stationary structure of the SGRP with different levels of clustering were explored (Table 2) to evaluate the hypothesis of rainfall (non)stationarity in time (Fig. 7b) and to explore the dominant factors controlling the rainfall process in our test case. These include NoCluster and NoCluster-Rand (no classification), ACP (classification into 8 ACP types), Season (classification into 4 seasons), Season6 and Season6-Rand (classification into 6 seasons), Monthly (classification into 12 months), Season-ACP (classification into $8 \times 4 = 32$ classes), Season6-ACP (classification into 8×6 classes), Season6-ACP-ND (same as Season6-ACP but without inclusion of topographic drift), and Season6-ACP-GC (same as Season6-ACP but conditioned on the gauge data). Here, the dominant control processes of interest are (1) ACPs, (2) seasonality, and (3) sequencing of

Table 2 Description of the several SRGP model classification levels implemented

Model name	ACP clustering	Conditioned simulation	Topography external drift	Rainy days sequence	Description
NoCluster	No	No	Yes	Observed	No classification
NoCluster-Rand	No	No	Yes	Synthetic	No classification
ACP	Yes	No	Yes	Observed	W/NW/SW/N, E-NE, S-SE, A-HYA, C, HYC, UC, UA
Season	No	No	Yes	Observed	Jan, Feb, Mar, Apr, May, Jun, Jul, Aug, Sep, Oct, Nov, Dec
Season6	No	No	Yes	Observed	Jan, Feb, Mar, Apr, May, Jun, Jul, Aug, Sep, Oct, Nov, Dec
Season6-Rand	No	No	Yes	Synthetic	Jan, Feb, Mar, Apr, May, Jun, Jul, Aug, Sep, Oct, Nov, Dec
Monthly	No	No	Yes	Observed	Jan, Feb, Mar, Apr, May, Jun, Jul, Aug, Sep, Oct, Nov, Dec
Season-ACP	Yes	No	Yes	Observed	Each ACP is classification by seasons
Season6-ACP	Yes	No	Yes	Observed	Each ACP is classification by season6
Season6-ACP-ND	Yes	No	No	Observed	Each ACP is classification by season6
Season6-ACP-GC	Yes	Yes	Yes	Synthetic	Each ACP is classification by season6

rainy days. Accordingly, the season, season6 and monthly models incorporate only seasonality, the ACP, season-ACP, season6-ACP models incorporate ACPs (with and without seasonality) and the NoCluster-Rand and season6-Rand models use randomization of the rainy day sequences. The model parameters were calibrated using the available data (without a validation period) so as to minimize the possibility of biasing the model toward a specific climate persistence condition (long wet or dry cycles). For each conceptual SRGP model structure, we generated one hundred rainfall field simulations (replicates) with a spatial resolution of 2.5 km for each of the rainy days from 1959–2007 (11735 days $\times$ 100 realizations). These simulations were "unconditioned" (not conditioned on the rain gauge data), with the exception of those for the season6-ACP-GC case, for which the simulations *were* conditioned on the rainfall measurements. This model case should be very close to reality and was used as a benchmark case to compare the spatial distributions of rainfall obtained with all other models.

6.1 Reproduction of Climatology

6.1.1 Climatological Pattern of Mean Areal Rainfall

Here, we compare the areal-average climatological rainfall (ACR) plot for the different SGRP models (Table 2) with the observed ACR data (Fig. 8). Figure 8a compares the ACR plots for the season-ACP and season6-ACP cases. Both cases involve ACP clustering of the rainy days, but each uses a different time-resolution for seasonal classification: season-ACP cluster into four seasons, and season6-ACP into six periods of different time lengths (Table 2). Note that Season6 better represents the seasonal transitions from spring to summer and from autumn to winter and the driest months (July and August) in the UppGb. Clearly, season6-ACP provides a better fit to the observed ACR data. To further explore the hypothesis regarding role of the ACPs, the ACR plots obtained using the season, season6 and monthly classification models are examined. None of these models include classification by ACP, but differ in the seasonal classification of rainy days (Table 2). Figure 8b shows that the higher the number of classification levels, the better the fit to the climatological pattern. Moreover, the fit for season6 is very similar to that obtained for season6-ACP (Fig. 8a). Given that the only difference between season6 and season6-ACP is the ACP clustering of rainy days, this seems to suggest that ACPs provide only a weak control in the reproduction of average climatological rainfall. This is an expected result due to the seasonality of the rainfall by ACP as shown in Fig. 7b. To shed more light on this, we remove the seasonal classification of the rainy days (Fig. 8c) and show the computed ACR series for NoCluster and ACP (only clustering by ACPs) models (both of which used the same sequence of rainy days). The result shows that the last two models are biased, even though they partly reproduce the climatological pattern. This tends to support the finding regarding the role played by the ACP information in climatology of areal average rainfall, and illustrates the importance of (1) using the correct sequence of rainy days, and (2) the clustering by seasons in the simulation procedure.

To gain a better understanding of this point, two new SRGP models termed NoCluster-Rand and season6-Rand are developed, each of which uses a synthetic

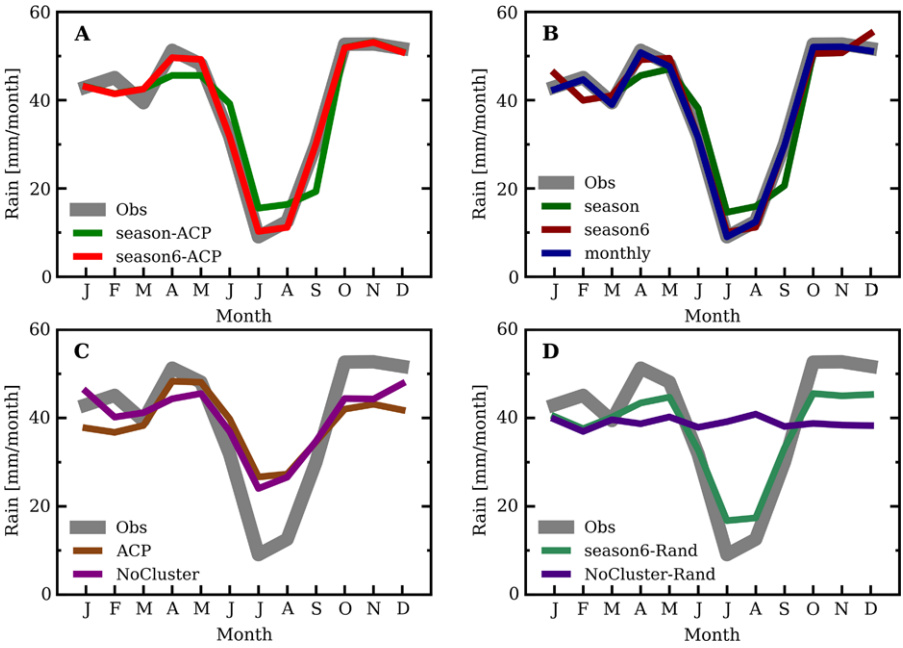

Fig. 8 Climatology plots of spatial average precipitation for different conceptual SRGPs classification models. Observed climatology is shown using a *bold gray line*. (**A**) Comparison between *season-ACP* and *season6-ACP*; both models have the same ACP aggregation model but *season6-ACP* has a higher number of seasonal divisions for classifying the rainy days. (**B**) Model response when the ACP classification is removed to leave only classification by *season*, *season6* and *monthly*. (**C**) Effect of removing the seasonality (leaving only *ACP*) and no classification (*NoCluster*). (**D**) Comparison between *season6-Rand* and *NoCluster-Rand* to demonstrate the effect of randomizing the sequence of rainy days for a given ACP sequence

sequence of rainy days for parameter calibration, obtained by randomly ordering the rainy days for the whole time period. Neither of these models includes ACP clustering, and only in season6-rand is a seasonal classification of the rainy days considered. Figure 8d shows that only season6-Rand, which accounts for seasonal clustering, displays some seasonal behavior, whereas the ACR plot for the NoCluster-Rand case only reproduces the mean precipitation value with no climatological pattern. Clearly, seasonal classification of the number of rainy days plays a key role in the climatology of rainfall.

6.1.2 Interannual Variability in the Climatological Pattern

Although the results above indicate that ACPs play a weak role in controlling mean annual climatology, it is also important to reproduce the *inter-annual variability* in the climatological pattern. The observed climatological rainfall variability (Fig. 9) is shown as a modified box plot (instead of interquartile range we show the 5th, 10th, 90th, 95th quantiles) for every month. The plot also shows the simulated climatological rainfall variability for the *season6* and *season6-ACP* models. It is clear that the

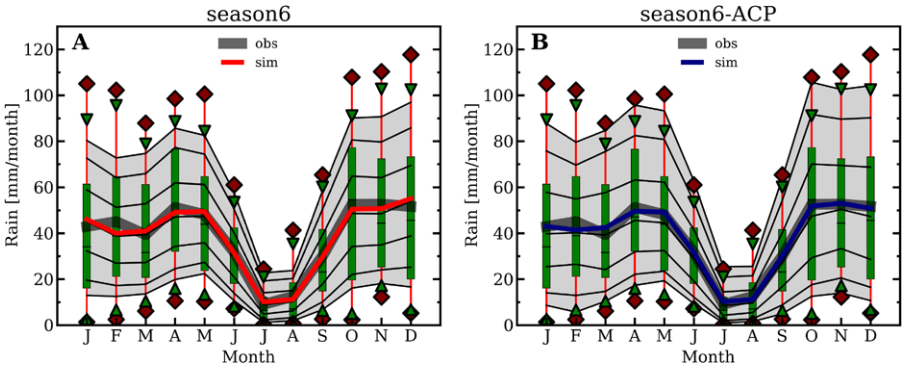

Fig. 9 Plots showing extent of inter-annual variability of the climatology of spatial average precipitation. Observed variability is represented by modified box plots showing has two upper percentile limits (95th and 90th represented by the *upper diamond* and *triangle*, respectively) and two lower percentile limits (5th and 10th represented by the *lower diamond* and *triangle*, respectively). The observed mean climatology is represented by the *bold gray line*. Simulated variability (averaged over 100 realizations) is shown by different quantile intervals (5, 10, 25, 50, 75, 90, 95). The two plots represent different conceptual SRGP models: (**A**) *season6*, and (**B**) *season6-ACP*. *Red* and *blue lines* represent the respective simulated ensemble mean climatologies

ACP-based model reproduces the interannual variability much better, revealing the importance of ACP-based clustering of rainy days.

6.1.3 Climatological Pattern of Rainfall at the Gauges

The results presented in Sect. 6.1.1 allow us for determining whether basin average rainfall value is reproduced, and to investigate dominant processes at the catchment scale. To evaluate the ability to simulate spatial nonstationarity of rainfall, the pixels coinciding with the locations of meteorological stations in the basin are selected from the simulated field. The performance of the season6-ACP and season6-ACP-ND models are examined, both of which include ACP clustering and seasonal classification (Table 2), but which differ in that the topographic external drift is only included in season6-ACP. Figure 10 displays the observed average annual climatology of rainfall for meteorological stations located at different points in the UppGb, with elevations of 625, 740, 810, and 984 m a.s.l., respectively. The plot also shows the results for the 100 simulation ensembles, along with their confidence intervals (5 % to 95 %). The inclusion of the orographic effect on rainfall improves the results in areas with high and low elevations. In average elevation zones, both models (i.e., Drift and No Drift) yield the same results. The confidence intervals for the No Drift (pink shaded areas in Fig. 10) are similar regardless of the rain gauge elevation. The observed rainfall that increases with elevation is captured by the Drift model.

6.1.4 Climatology of Spatial Rainfall Distribution

Here, we compare the climatological spatial patterns of rainfall for the *season6-ACP* and *season6-ACP-ND* models with the results obtained using the *season6-ACP-GC*

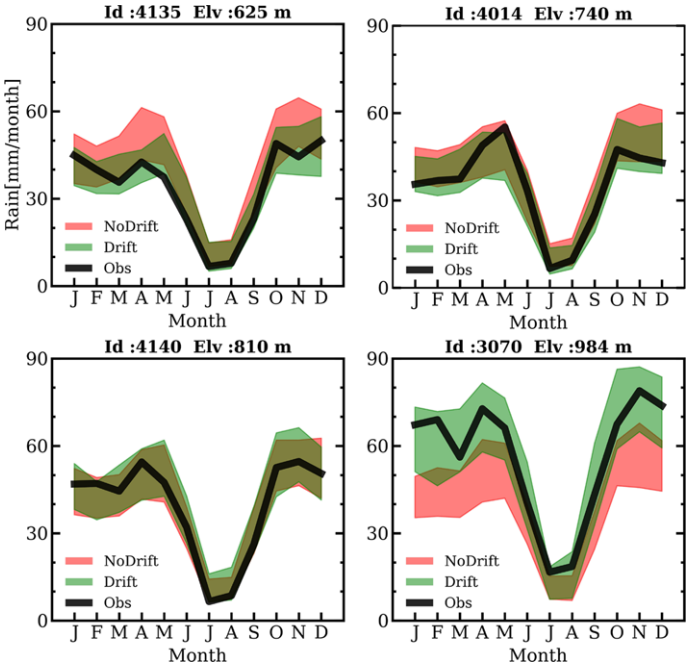

Fig. 10 Climatology of rainfall at three different locations for a model that includes the spatial drift (*season6-ACP*) and for one that does not (*season6-ACP-ND*). Elevation increases from left to right. *Shaded areas* represent variability over the 100 simulation ensembles, along with their confident intervals (5 % to 95 %). The *dark green shaded area* corresponds to the intersection zone between the two models

model, in which the simulations are conditioned on the observed rain gauge data (and hence provide the best possible estimate of the spatial distribution of rain at the desired resolution). Figure 11 compares the normalized error fields for the wettest (May) and driest (August) months (Fig. 11 middle and lower panels), along with the digital terrain model (DTM) for the UppGb. In the wettest case, the mean rainfall field for *season6-ACP* bears a greater resemblance to the DTM than do the models that do not include the rainfall orographic effect. In contrast, the driest case shows no significant difference between *season6-ACP* and *season6-ACP-ND*. This contrasting behavior may be explained in terms of the spatial correlation structure of rain during May and August; rainfall in May is characterized by large-scale stratiform precipitation fronts slowly crossing the whole UppGb, whereas rainfall in August is mainly due to small/local convective cells of short duration.

6.2 Spatial Distribution of Rainfall

Next, we determine whether the simulated spatial distribution of rainfall matches the observations. To this end, we use the quantile–quantile (Q–Q) plot to compare the observed and the simulated rainfall for (1) the selected rain gauge sites, and (2) the basin averaged rainfall. Here, we only use the *season6-ACP model*.

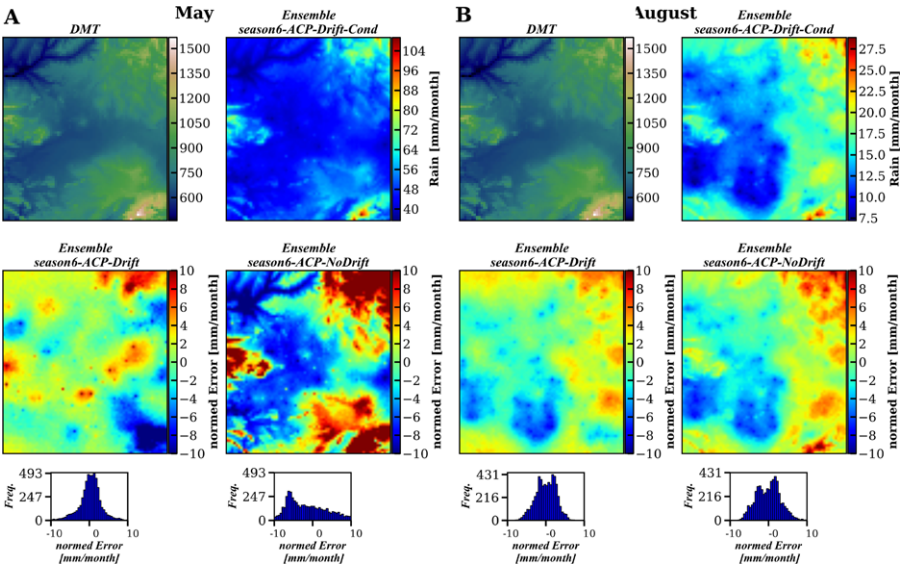

Fig. 11 Plots of the mean ensemble spatial rainfall fields for (**A**) May, the wettest month, and (**B**) August, the driest month. Each panel presents the digital terrain model (*upper left panel*) of the Upper Guadiana Basin and the comparison between three different conceptual SGRP models with the same classification level (*season6-ACP*), but with different conditional information. The *season6-ACP-Drift-Cond* results (*upper right panel*) are conditioned to the historical time series observations and incorporates topographic spatial drift. The *season6-ACP-Drift* results are unconditional simulations and include spatial topographic drift. The *season6-ACP-NoDrift* results are unconditional simulations and do not include spatial drift. In the *middle* and *bottom panels* are the normed error difference field and histograms between *season6-ACP-Drif-Cond* and *season6-ACP-Drift* (*left middle* and *bottom panel*) and *season6-ACP-NoDrift* (*right middle* and *bottom panel*)

6.2.1 Rainfall Distributions at the Gauges

Figure 12 shows the Q–Q plots corresponding to several meteorological stations distributed throughout the UppGb. In general, the rainfall distributions appear to be well reproduced regardless of the elevation of the rain gauge. This is especially true for values of precipitation below 30 mm. Higher values show increased dispersion (the shaded area ranges from 5 % to 95 % of the confident interval) and a tendency to overestimate large rainfall values. Since the model uses empirical rainfall distributions with a finite sample size, the above problems could be resolved by (1) increasing the sample size using any interpolation technique or by (2) modifying the limits of the normal score distribution. In other words, the amount of (observed) data used to define the normal score transformation, and the amount of simulated data values must be large enough to correspond to the recurrence time of the extreme values that we wish to simulate.

6.2.2 Distribution of Areal-Average Rainfall

We evaluate the Q–Q plots for areal-average rainfall for three different time scales: (1) daily, (2) monthly accumulated, and (3) yearly accumulated. The results (Fig. 13)

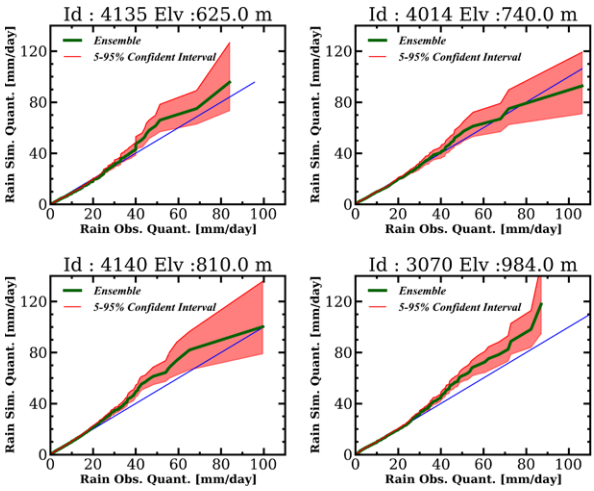

Fig. 12 Quantile–Quantile plots comparing distributions of observed and simulated daily rainfall intensities at four different rain gauge locations

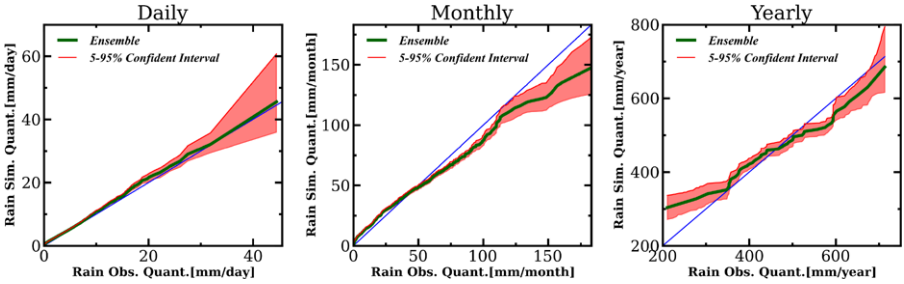

Fig. 13 Quantile–Quantile plots comparing distributions of observed and the simulated daily (*left*), monthly accumulated (*center*) and yearly accumulated (*right*) spatially averaged precipitation

are fairly good for daily rainfall, but not so good for the two other cases. Nevertheless, the yearly Q–Q plot shows that the model overestimates the minimum values (driest years) and underestimates the maximum values (wettest years). This is mainly due to the choice of the gamma function $\Gamma_{\hat{\mu}_{zj}}$ (Eq. (7)) used to represent the pdf of the spatial average rainfall. The gamma function fits the mean and the mode values fairly well, but is not so good for the tails of the distribution (Fig. 2). This effect could be resolved by other distributions that better represent the extreme values (Vrac and Naveau 2007; Furrer and Katz 2008; Solari and Losada 2012), an issue we intend to explore further in an on-going work.

6.3 Intermittence of Rainfall

Figure 14 shows an example of the final rainfall fields obtained by applying the methodology for different percentage of fractional area covered by rain: 5, 25, 50, and 80. Results are shown for the *season6-ACP* model including the representation of external drift with elevation. The plots show that the SIS method realistically reproduces the intermittence process in terms of the clustering of regions with rainfall.

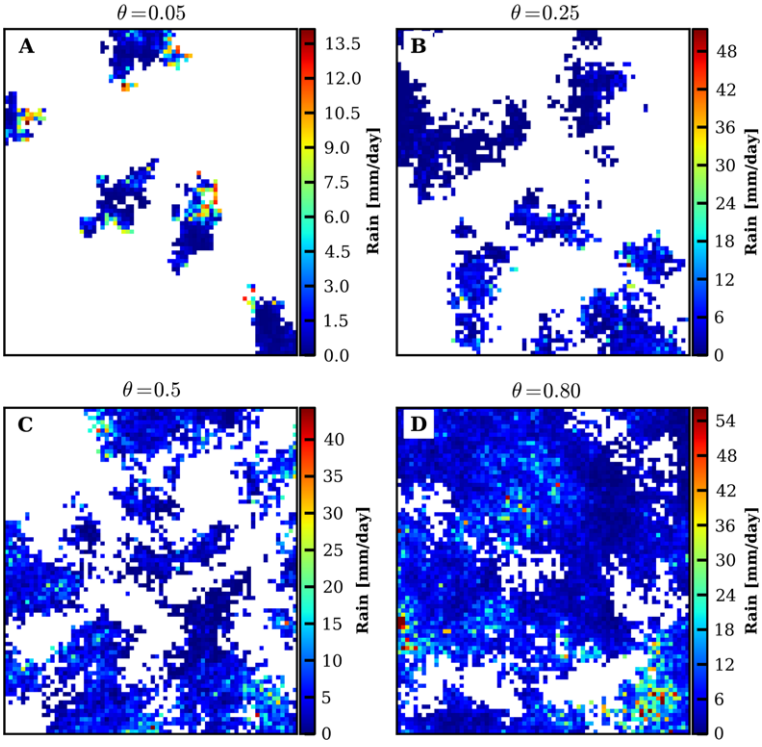

Fig. 14 Examples of daily rainfall fields generated for different days with variable fraction of rain-covered area: (**A**) 0.05, (**B**) 0.25, (**C**) 0.5, and (**D**) 0.8

However, the fields tend to show sharp transitions between rain and no rain areas because of the assumption of independence between the intensity and intermittence processes.

7 Discussion and Conclusions

A method for simulating daily rainfall fields with sufficient spatial resolution is presented, to be used in spatially distributed hydrological modeling. The approach incorporates several sources of information, and simulates major nonstationarity features of the rainfall fields. By exploiting information regarding the sequence of ACPs it is possible to obtain time stationary sequences of SRGPs. This allows the model to exploit invaluable information regarding climate variability/change provided by GCMs. Consequently, the approach can be used for developing multiple stochastic ensembles of downscaled rainfall fields for use in CCIS assessments (including uncertainty analysis). Further, the approach has the ability to generate both conditional and unconditional rainfall field simulations. As a result, the model can be used to fill observation data gaps in the historical rainfall data sets.

The model is tested using the Upper Guadiana Basin in Spain and found to provide an accurate reproduction of the major spatiotemporal features of rainfall needed

for hydrological modeling and water resource evaluations. The incorporation of spatial drift related to orographic precipitation significantly improved the results. The incorporation of seasons enabled the reproduction of the observed climatology of spatial averaged rainfall. ACP clustering improved the reproduction of the interannual climatological variability. Nevertheless, certain aspects of the model need to be improved. First of all, the assumption of independence between rainfall amount and the rainfall intermittence fields produces sharp transitions between the areas of rain and no rain in the daily rainfall fields obtained. This is an important issue that should be addressed in the future. Some authors (Bell 1987; Guillot 1999; Kleiber et al. 2012) use a threshold-based method to simulate rainfall occurrence, which employs the same latent Gaussian process that simulates rainfall amounts. Comparing both methods, De Oliveira (2004) suggests that the application of one of the two models depends mainly on the precipitation patterns of the specific region under study. From the hydrological point of view, the correlation between rainfall intensity and intermittence should be better represented. Second, the Q–Q plot analysis indicates that extreme rainfall values and their frequency of occurrence are overestimated.

In an on-going work, we are evaluating the usefulness of the approach for downscaling rainfall fields in the context of climate change. Such analysis is supported by the expectation that climate change will affect the frequency of the ACPs, and hence the precipitation regimes (Trenberth 2011). To establish the robustness of such applications, it is necessary to ascertain whether the SRGP model parameters can be assumed as stationary for the future. Naturally, for climate impact analysis *some* assumptions should be made. However, it is important to evaluate the degree to which the results could be affected by these assumptions. Moreover, when the approach is used in the context of distributed catchment modeling, the spatiotemporal variability of the precipitation can be expected to affect the response of the hydrological processes in different ways. It is therefore necessary to determine the degree of sensitivity of these responses to uncertainties in the SRGP model parameters.

Acknowledgements This research was undertaken as part of the European Union (FP6) funded Integrated Project WATCH through contract number 036946. The meteorological data were provided by the Spanish state meteorological agency (AEMET). The fourth author received partial support from the Spanish Ministry of Science and Innovation (MEC) and from the Australian Research Council through the Centre of Excellence for Climate System Science (grant number CE110001028). Comments by the editor and referees are gratefully acknowledged.

References

Barancourt C, Creutin JD, Rivoirard J (1992) A method for delineating and estimating rainfall fields. Water Resour Res 28(4):1133–1144. doi:10.1029/91WR02896

Bardossy A, Plate EJ (1992) Space-time model for daily rainfall using atmospheric circulation patterns. Water Resour Res 28(5):1247–1259. doi:10.1029/91WR02589

Barros AP, Lettenmaier DP (1994) Dynamic modeling of orographically induced precipitation. Rev Geophys 32(3):265–284. doi:10.1029/94RG00625

Bell TL (1987) A space-time stochastic model of rainfall for satellite remote-sensing studies. J Geophys Res 92(D8):9631–9643. doi:10.1029/JD092iD08p09631

Bellone E, Hughes JP, Guttorp P (2000) A hidden Markov model for downscaling synoptic atmospheric patterns to precipitation amounts. Clim Res 15(1):1–12. doi:10.3354/cr015001

Buishand TA, Brandsma T (2001) Multisite simulation of daily precipitation and temperature in the Rhine basin by nearest-neighbor resampling. Water Resour Res 37(11):2761–2776. doi:10.1029/2001WR000291

Burton A, Fowler HJ, Kilsby CG, O'Connell PE (2010) A stochastic model for the spatial-temporal simulation of nonhomogeneous rainfall occurrence and amounts. Water Resour Res 46(11):W11501. doi:10.1029/2009WR008884

Bader DC, Covey C, Gutowski WJ Jr., Held IM, Kunkel KE, Miller RL, Tokmakian RT, Zhang MH (CCSP) (2008) Climate Models: An Assessment of Strengths and Limitations. A Report by the US Climate Change Science Program and the Subcommittee on Global Change Research Department of Energy. Office of Biological and Environmental Research, Washington. 124 pp

Chandler RE, Wheater HS (2002) Analysis of rainfall variability using generalized linear models: a case study from the west of Ireland. Water Resour Res 38(10):1192. doi:10.1029/2001WR000906

Cho H-K, Bowman KP, North GR (2004) A comparison of gamma and lognormal distributions for characterizing satellite rain rates from the tropical rainfall measuring mission. J Appl Meteorol 43(11):1586–1597. doi:10.1175/JAM2165.1

Corte-Real J, Xu H, Qian B (1999) A weather generator for obtaining daily precipitation scenarios based on circulation patterns. Clim Res 13(1):61–75. doi:10.3354/cr013061

Cowpertwait PS (1995) A generalized spatial-temporal model of rainfall based on a clustered point process. Proc R Soc Lond Ser A, Math Phys Sci 450:163–175

Cowpertwait PS (2010) A spatial-temporal point process model with a continuous distribution of storm types. Water Resour Res 46(12):W12507. doi:10.1029/2010WR009728

Dai A (2006) Precipitation characteristics in eighteen coupled climate models. J Climate 19(18):4605–4630. doi:10.1175/JCLI3884.1

De Oliveira V (2004) A simple model for spatial rainfall fields. Stoch Environ Res Risk Assess 18:131–140. doi:10.1007/s00477-003-0146-4

Deutsch C, Journel A (1997) GSLIB: geostatistical software library and user's guide. Oxford University Press, London. 384 pp

Doneaud A, Ionescu-Niscov S, Priegnitz DL, Smith PL (1984) The area-time integral as an indicator for convective rain volumes. J Clim Appl Meteorol 23(4):555–561. http://dx.doi.org/10.1175/1520-0450(1984)023<0555:TATIAA>2.0.CO;2

Ebtehaj M, Foufoula-Georgiou E (2010) Orographic signature on multiscale statistics of extreme rainfall: a storm-scale study. J Geophys Res 115(D23):D23112. doi:10.1029/2010JD014093

Ehret U, Zehe E, Wulfmeyer V, Warrach-Sagi K, Liebert J (2012) HESS opinions "Should we apply bias correction to global and regional climate model data?". Hydrol Earth Syst Sci 16(9):3391–3404. doi:10.5194/hess-16-3391-2012

Eltahir EA, Bras RL (1993) Estimation of the fractional coverage of rainfall in climate models. J Climate 6(4):639–644. http://dx.doi.org/10.1175/1520-0442(1993)006<0639:EOTFCO>2.0.CO;2

Fowler HJ, Blenkinsop S, Tebaldi C (2007) Linking climate change modelling to impacts studies: recent advances in downscaling techniques for hydrological modelling. Int J Climatol 27(12):1547–1578. doi:10.1002/joc.1556

Fowler HJ, Kilsby CG, O'Connell PE (2000) A stochastic rainfall model for the assessment of regional water resource systems under changed climatic condition. Hydrol Earth Syst Sci 4(2):263–281. doi:10.5194/hess-4-263-2000

Fowler H, Kilsby C, O'Connell P, Burton A (2005) A weather-type conditioned multi-site stochastic rainfall model for the generation of scenarios of climatic variability and change. J Hydrol 308(1–4):50–66. doi:10.1016/j.jhydrol.2004.10.021

Furrer EM, Katz RW (2008) Improving the simulation of extreme precipitation events by stochastic weather generators. Water Resour Res 44(12):W12439. doi:10.1029/2008WR007316

Gleckler PJ, Taylor KE, Doutriaux C (2008) Performance metrics for climate models. J Geophys Res 113(D6):D06104. doi:10.1029/2007JD008972

Gómez-Hernández J, Cassiraga E (1994) Theory and practice of sequential simulation. Geostatistical simulations. In: Armstrong M, Dowd P (eds) Geostatistical simulations. Kluwer Academic, Dordrecht, pp 111–121

Gómez-Hernández JJ, Srivastava RM (1990) ISIM3D: an ANSI-C three-dimensional multiple indicator conditional simulation program. Comput Geosci 16(4):395–440. doi:10.1016/0098-3004(90)90010-Q

Goodess CM, Palutikof JP (1998) Development of daily rainfall scenarios for southeast Spain using a circulation-type approach to downscaling. Int J Climatol 18(10):1051–1083. 3.0.CO; 2-1. doi:10.1002/(SICI)1097-0088(199808)18:10<1051::AID-JOC304>3.0.CO;2-1

Goovaerts P (1997) Geostatistics for natural resources evaluation. Oxford University Press, London. 496 pp
Guillot G (1999) Approximation of Sahelian rainfall fields with meta-Gaussian random functions. Stoch Environ Res Risk Assess 13:100–112. doi:10.1007/s004770050034
Gupta VK, Waymire EC (1993) A statistical analysis of mesoscale rainfall as a random cascade. J Appl Meteorol 32(2):251–267. http://dx.doi.org/10.1175/1520-0450(1993)032<0251:ASAOMR>2.0.CO;2
Hay LE, McCabe GJ, Wolock DM, Ayers MA (1991) Simulation of precipitation by weather type analysis. Water Resour Res 27(4):493–501. doi:10.1029/90WR02650
Jenkinson A, Collison F (1977) An initial climatology of gales over the North Sea. Synoptic climatology branch memorandum 62
Jodar J, Carrera J, Cruz A (2010) Irrigation enhances precipitation at the mountains downwind. Hydrol. Earth Syst. Sci 14(10):2003–2010. doi:10.5194/hess-14-2003-2010
Johnson F, Sharma A (2011) Accounting for interannual variability: a comparison of options for water resources climate change impact assessments. Water Resour Res 47(4). doi:10.1029/2010wr009272
Johnson F, Sharma A (2012) A nesting model for bias correction of variability at multiple time scales in general circulation model precipitation simulations. Water Resour Res 48(W01504):16. doi:10.1029/2011WR010464
Jones PD, Hulme M, Briffa KR (1993) A comparison of Lamb circulation types with an objective classification scheme. Int J Climatol 13(6):655–663. doi:10.1002/joc.3370130606
Jothityangkoon C, Sivapalan M, Viney NR (2000) Tests of a space-time model of daily rainfall in southwestern Australia based on nonhomogeneous random cascades. Water Resour Res 36(1):267–284. doi:10.1029/1999WR900253
Kalnay E, Kanamitsu M, Kistler R, Collins W, Deaven D, Gandin L et al (1996) The NCEP/NCAR 40-year reanalysis project. Bull Am Meteorol Soc 77(3):437–471. http://dx.doi.org/10.1175/1520-0477(1996)077<0437:TNYRP>2.0.CO;2
Kang B, Ramirez JA (2010) A coupled stochastic space-time intermittent random cascade model for rainfall downscaling. Water Resour Res 46(10):W10534. doi:10.1029/2008WR007692
Kedem B, Chiu LS (1987) On the lognormality of rain rate. Proc Natl Acad Sci USA 84(4):901–905
Kedem B, Pavlopoulos H (1991) On the threshold method for rainfall estimation: choosing the optimal threshold level. J Am Stat Assoc 86(415):626–633
Kleiber W, Katz RW, Rajagopalan B (2012) Daily spatiotemporal precipitation simulation using latent and transformed Gaussian processes. Water Resour Res 48(1):W01523. doi:10.1029/2011WR011105
Kundu PK, Siddani RK (2007) A new class of probability distributions for describing the spatial statistics of area-averaged rainfall. J Geophys Res 112(D18):D18113. doi:10.1029/2006JD008042
Kursinski AL, Zeng X (2006) Areal estimation of intensity and frequency of summertime precipitation over a midlatitude region. Geophys Res Lett 33(22):L22401. doi:10.1029/2006GL027393
Kyriakidis P, Journel A (1999) Geostatistical space-time models: a review. Math Geol 31:651–684. doi:10.1023/A:1007528426688
Kyriakidis P, Miller N, Kim J (2004) A spatial time series framework for simulating daily precipitation at regional scales. J Hydrol 297(1–4):236–255. doi:10.1016/j.jhydrol.2004.04.022
Lanza LG (2000) A conditional simulation model of intermittent rain fields. Hydrol Earth Syst Sci 4(1):173–183. doi:10.5194/hess-4-173-2000
Maraun D, Wetterhall F, Ireson AM, Chandler RE, Kendon EJ, Widmann M, Brienen S, Rust HW, Sauter T, Themeßl M, Venema VKC, Chun KP, Goodess CM, Jones RG, Onof C, Vrac M, Thiele-Eich I (2010) Precipitation downscaling under climate change: recent developments to bridge the gap between dynamical models and the end user. Rev Geophys 48(3):RG3003. doi:10.1029/2009RG000314
Mehrotra R, Sharma A (2007) A semi-parametric model for stochastic generation of multi-site daily rainfall exhibiting low-frequency variability. J Hydrol 335(1–2):180–193. doi:10.1016/j.jhydrol.2006.11.011.
Mehrotra R, Sharma A (2009) Evaluating spatio-temporal representations in daily rainfall sequences from three stochastic multi-site weather generation approaches. Adv Water Resour 32(6):948–962. doi:10.1016/j.advwatres.2009.03.005
Mehrotra R, Sharma A (2010) Development and application of a multisite rainfall stochastic downscaling framework for climate change impact assessment. Water Resour Res 46. doi:10.1029/2009WR008423
Mejía JM, Rodríguez-Iturbe I (1974) On the synthesis of random field sampling from the spectrum: an application to the generation of hydrologic spatial processes. Water Resour Res 10(4):705–711. doi:10.1029/WR010i004p00705

Northrop P (1998) A clustered spatial-temporal model of rainfall. Proc R Soc A, Math Phys Eng Sci 454(1975):1875–1888

Onibon H, Lebel T, Afouda A, Guillot G (2004) Gibbs sampling for conditional spatial disaggregation of rain fields. Water Resour Res 40(8):W08401. doi:10.1029/WR010i004p00705

Perica S, Foufoula-Georgiou E (1996) Model for multiscale disaggregation of spatial rainfall based on coupling meteorological and scaling descriptions. J Geophys Res 101(D21):26347–26361. doi:10.1029/96JD01870

Randall DA, Wood RA, Bony S, Colman R, Fichefet T, Fyfe J, Kattsov V, Pitman A, Shukla J, Srinivasan J, Stouffer RJ, Sumi A, Taylor KE (2007) Cilmate models and their evaluation. In: Solomon S, Qin D, Manning M, Chen Z, Marquis M, Averyt KB, Tignor M, Miller HL (eds) Climate change 2007: the physical science basis. Contribution of working group I to the fourth assessment report of the intergovernmental panel on climate change. Cambridge University Press, Cambridge

Rodríguez-Iturbe I, Cox DR, Eagleson PS (1986) Spatial modelling of total storm rainfall. Proc R Soc Lond Ser A, Math Phys Sci 403:27–50. 1824

Schertzer D, Lovejoy S (1987) Physical modeling and analysis of rain and clouds by anisotropic scaling multiplicative processes. J Geophys Res 92(D8):9693–9714. doi:10.1029/JD092iD08p09693

Shah S, O'Connell P, Hosking J (1996) Modelling the effects of spatial variability in rainfall on catchment response. 1. Formulation and calibration of a stochastic rainfall field model. J Hydrol 175(1–4):67–88. doi:10.1016/S0022-1694(96)80006-0

Sharma A, Mehrotra R (2010) Rainfall generation. Geophys monogr ser, vol 191. AGU, Washington, pp 215–246. doi:10.1029/2010GM000973

Sherman M (2011) Spatial statistics and spatio-temporal data: covariance functions and directional properties. Wiley, New York. 294 pp

Solari S, Losada MA (2012) A unified statistical model for hydrological variables including the selection of threshold for the peak over threshold method. Water Resour Res 48(10):W10541. doi:10.1029/2011WR011475

Srikanthan R, McMahon TA (2001) Stochastic generation of annual, monthly and daily climate data: a review. Hydrol Earth Syst Sci 5(4):653–670. doi:10.5194/hess-5-653-2001

Stern RD, Coe R (1984) A model fitting analysis of daily rainfall data. J R Stat Soc, Ser A, Stat Soc 147(1):1–34

Teo C-K, Grimes DI (2007) Stochastic modelling of rainfall from satellite data. J Hydrol 346(1–2):33–50. doi:10.1016/j.jhydrol.2007.08.014

Trenberth K (2011) Changes in precipitation with climate change. Clim Res 47(1–2):123–138. doi:10.3354/cr00953

Trenberth KE, Dai A, Rasmussen RM, Parsons DB (2003) The changing character of precipitation. Bull Am Meteorol Soc 84(9):1205–1217. doi:10.1175/BAMS-84-9-1205

Vrac M, Naveau P (2007) Stochastic downscaling of precipitation: from dry events to heavy rainfalls. Water Resour Res 43(7):W07402. doi:10.1029/2006WR005308

Waymire E, Gupta VK, Rodríguez-Iturbe I (1984) A spectral theory of rainfall intensity at the meso-beta scale. J Water Resour Res 20(10):1453–1465. doi:10.1029/WR020i010p01453

Wheater H, Chandler R, Onof C, Isham V, Bellone E, Yang C, Lekkas D, Lourmas G, Segond ML (2005) Spatial–1temporal rainfall modelling for flood risk estimation. Stoch Environ Res Risk Assess 19:403–416. doi:10.1007/s00477-005-0011-8

Wilks DS (1998) Multisite generalization of a daily stochastic precipitation generation model. J Hydrol 210(1–4):178–191. doi:10.1016/S0022-1694(98)00186-3

Yang C, Chandler RE, Isham VS, Wheater HS (2005) Spatial-temporal rainfall simulation using generalized linear models. Water Resour Res 41(11):W11415. doi:10.1029/2004WR003739

Yang W, Bárdossy A, Caspary H-J (2010) Downscaling daily precipitation time series using a combined circulation- and regression-based approach. Theor Appl Climatol 102:439–454. doi:10.1007/s00704-010-0272-0

Zhang Z, Switzer P (2007) Stochastic space-time regional rainfall modeling adapted to historical rain gauge data. Water Resour Res 43(3):W03441. doi:10.1029/2005WR004654